Nuclear Mathematical and Computational Sciences: A Century in Review, A Century Anew
Gatlinburg, Tennessee, April 6-11, 2003, on CD-ROM, American Nuclear Society, LaGrange Park, IL (2003)

AN INTRA-NODAL FLUX EXPANSION FOR A HETEROGENEOUS COARSE MESH DISCRETE ORDINATES METHOD

Scott W. Mosher and Farzad Rahnema
Nuclear and Radiological Engineering and Health Physics Programs
George W. Woodruff School of Mechanical Engineering
Georgia Institute of Technology
Atlanta, Georgia 30332
gt3522a@prism.gatech.edu; farzad.rahnema@nre.gatech.edu

ABSTRACT

The extension of the variational heterogeneous coarse mesh method due to Ilas and Rahnema to two-dimensional (2-D) geometries is hindered by the sheer number of response function (RF) calculations to be performed in realistic reactor core problems. In this paper, we present some preliminary work aimed at reducing the number of RFs required to achieve a high degree of accuracy in the global flux solution. Specifically, the original intra-nodal angular flux RFs (surface Green's functions) are replaced by responses to a set of node-edge incident fluxes which, in 1-D problems, are the normalized discrete Legendre polynomials in *mu* (cosine of the angle between the neutron direction and the *x*-axis). Numerical results are presented for three simple one-speed, slab-geometry cores, with varying degrees of heterogeneity, using S-12 quadrature. For these problems, a substantial savings in the number of RF calculations was obtained.

Key Words: Heterogeneous Coarse Mesh Methods, Variational Methods, Discrete Ordinates Methods, and Angular Flux Expansion.

1. INTRODUCTION

In the past two decades, a handful of heterogeneous coarse mesh (*i.e.*, core level) neutronics methods have appeared in the literature (*e.g.*, [1-6]). The essential characteristic of these methods is the avoidance of fuel assembly homogenization, as is necessary with conventional nodal methods [7, 8]. For the most part, these heterogeneous methods involve the following phases (note that the terms node and coarse mesh are used interchangeably):

1. compute the intra-nodal flux distributions (responses) caused by node-edge and (optionally) in-volume sources using fixed source calculations on single, unique coarse meshes (*e.g.*, one fuel assembly plus half the surrounding coolant gap);

2. solve for the source distributions in the global calculation using the response functions (RFs) and, perhaps, by employing variational techniques; and

3. construct the global flux solution by a linear superposition of the response functions with coefficients determined by the source information.

The three phases are, to a degree, similar to the homogenization, nodal calculation, and de-homogenization steps performed in conventional nodal core calculations. The fundamental difference is the way in which a node is characterized in the global calculation – by a set of homogenized cross sections and discontinuity factors in homogeneous methods, and by a set of response functions in heterogeneous methods.

There are several challenges to be faced when developing a heterogeneous method as described above. First, there is a need to ultimately base the method on transport theory at the lattice cell level due to the explicit modeling of heterogeneities within fuel assemblies. Second, the computation of a complete set of transport theory response functions for each unique node in a realistic core calculation is impractical (see Section 2). Third, an attempt to avoid homogenization at all levels requires directly using library cross sections, which tend to be in 30 to 45 energy groups for light water reactor (LWR) calculations. Finally, there is a practical need to allow the user to have control over the trade-off between accuracy and computational time.

With the aforementioned challenges in mind, the authors are currently working on extending a variational coarse mesh discrete ordinates method [6] from one to two-dimensional Cartesian geometry for LWR calculations. This paper summarizes initial effort that has been directed at developing an alternative intra-nodal flux expansion that allows a reduction in the number of response functions necessary to achieve a high degree of accuracy in the global solution. In Section 2, the original flux expansion idea is reviewed and a new one is presented. The numerical coarse-mesh method is described in Section 3. Numerical results for three one-dimensional (1-D), one-speed cores, with varying degrees of heterogeneity, are presented in Section 4. Conclusions and directions of future work can be found in Sections 5 and 6, respectively.

2. INTRA-NODAL FLUX EXPANSIONS

Previous work in diffusion [5] and transport theory [6] concerned the development of coarse-mesh methods in which a unique node is characterized by the solutions to fine mesh, fixed source problems with known incident flux boundary conditions. The incident flux distributions are required to be a set of orthogonal functions on the domain associated with the node edges. To be more specific, consider the 1-D discrete ordinates formulation [9] of the multigroup transport equation with isotropic scattering. In our approach, a single response function, denoted R, is the solution to

$$\mu_n \frac{d}{dx} R_{gn}(x) + \sigma_g(x) R_{gn}(x) = \frac{1}{2} \sum_{g'=1}^{G} \left[\left(\sigma_{0g' \to g}(x) + \frac{1}{k} \chi_g(x) \nu \sigma_{fg'}(x) \right) \sum_{n'=1}^{N} w_{n'} R_{g'n'}(x) \right] \quad (1)$$

within a single unique coarse mesh, with the boundary condition

$$R_{gn}(x) = \Gamma_{gn}(x) \text{ on } \partial V^* \quad (2)$$

where:
- n = ordinate index $(1, ..., N)$
- g = energy group index $(1, ..., G)$
- w_n = ordinate weights
- ∂V^* = $\{x = x_\ell$ and $\mu_n > 0;\ x = x_r$ and $\mu_n < 0\}$
- $x_{\ell/r}$ = left / right coarse mesh boundary

and the other notation is standard. Note that the fission source is scaled by a fixed factor $(1/k)$, which corresponds to an estimate of the core eigenvalue, so that Eqs. (1, 2) are posed as a fixed-source problem.

It is the choice of Γ in Eq. (2) which distinguishes recent developments from previous work. In [6], Γ was chosen as

$$\Gamma_{gn}(x) = \delta(x - x_b)\delta_{hg}\delta_{mn} \tag{3}$$

where: x_b $= x_\ell$ or x_r
h $=$ energy group index
m $=$ incident ordinate index

The first factor in Eq. (3) is a Dirac delta function, and the other two are Kronecker deltas. A solution to Eqs. (1-3) is called a surface Green's function (SGF) [10] with parameters h, m, x_b, and k. For a given value of k, there are a total of $G \times N$ of these functions (with a symmetric quadrature set) which collectively characterize a slab coarse mesh. A notation for the SGFs which involves the parameters, $G_{hm\rightarrow gn}(x_b \rightarrow x)$, is useful for writing down the expansion of the intra-nodal angular flux, ψ, in terms of a known incident angular flux, ξ, (and a given k) as

$$\psi_{gn}(x) = \sum_b \sum_h \sum_m \xi_{hm}(x_b) G_{hm\rightarrow gn}(x_b \rightarrow x) \tag{4}$$

This relationship holds because the transport equation is linear with respect to boundary conditions and the Γ's are orthogonal on ∂V^*. The expansion can be used as a means for quickly solving the transport equation when the SGFs have been pre-computed for each unique node [6].

The total number of surface Green's functions needed to characterize a unique coarse mesh is the same as the number of computational fine meshes in space, energy, and direction (discrete phase space locations) associated with incident fluxes. So when the expansion in Eq. (4) is extended to 2-D Cartesian geometry, the total number of SGFs grows geometrically. Consider the fine mesh boundaries of two hypothetical models of a single LWR coarse mesh presented in Table I

Table I. Phase Space Locations in the Boundaries of a Hypothetical Coarse Mesh

Dimension	1-D	2-D
space	2	100
energy	30	30
direction (S_8)	8	40

where the 2-D model consists of a 25×25 spatial fine mesh. For this case, the number of SGF calculations increases from 120 to 30,000 from 1 to 2-D, assuming that the 1 and 2-D lattice cells have left-to-right and diagonal symmetry, respectively. The situation looks even more bleak when it is noted that a LWR core may have 10 to 20 unique fuel assembly designs which have to be considered at a number of burnup, coolant density, fuel temperature, and control states. It can quickly be concluded that the computation of a complete set of response functions is impractical for routine calculations of realistic 2-D core problems.

Unfortunately, the surface Green's functions are not a good choice in which to expand the intra-nodal flux when an incomplete set of response functions has to be used. Simply neglecting individual SGFs will computationally close paths of entry into a coarse-mesh, which leads to significant errors in the global

solution (see Section 4). An alternative choice of incident flux boundary conditions, which will lead to a different set of response functions, has to be made.

We have recently used the discrete analog of the continuous Legendre polynomials to replace a single factor in the Γ of Eq. (3). The so-called discrete Legendre polynomials (DLPs) [11] will be denoted by $P_m(i,M)$, where m now represents the order of the polynomial and $i = 1, ..., M+1$ is the discrete variable. The normalized polynomials satisfy the orthogonality relation

$$\Big\langle P_\ell, P_m \Big\rangle \equiv \sum_{i=1}^{M+1} P_\ell(i,M) P_m(i,M) = \delta_{\ell m} \tag{5}$$

For example, when $M = 5$ the unnormalized DLPs, denoted $\tilde{P}$, are

$$\begin{aligned}
\tilde{P}_0(i,5) &= 1 \\
\tilde{P}_1(i,5) &= 1 - \frac{2}{5}i \\
\tilde{P}_2(i,5) &= 1 - \frac{6}{5}i + \frac{3}{10}i^{(2)} \\
\tilde{P}_3(i,5) &= 1 - \frac{12}{5}i + \frac{3}{2}i^{(2)} - \frac{1}{3}i^{(3)} \\
\tilde{P}_4(i,5) &= 1 - 4i + \frac{9}{2}i^{(2)} - \frac{7}{3}i^{(3)} + \frac{7}{12}i^{(4)} \\
\tilde{P}_5(i,5) &= 1 - 6i + \frac{21}{2}i^{(2)} - \frac{28}{3}i^{(3)} + \frac{21}{4}i^{(4)} - \frac{21}{10}i^{(5)}
\end{aligned} \tag{6}$$

where

$$i^{(j)} \equiv i(i-1)...(i-j+1) \tag{7}$$

is the j^{th} fading factorial of i. Setting

$$\Gamma_{gn}(x) = \delta(x - x_b)\delta_{hg} P_m(n - t, \frac{N}{2} - 1) \tag{8}$$

and solving Eqs. (1, 2, and 8) generates response functions $R_{mh\to gn}(x_b \to x)$ with parameters h, m, x_b, and k, which we call discrete Legendre polynomial response functions. In Eq. (8), $t = 0$ or $N/2$ to shift the discrete variable argument into the range $1, ..., N/2$ when necessary. Expansion coefficients are calculated as

$$a_{hm}(x_b) = \Big\langle \xi_{hn}(x_b), P_m(n - t, \frac{N}{2} - 1) \Big\rangle \tag{9}$$

and the intra-nodal flux is expanded as

$$\psi_{gn}(x) \cong \sum_b \sum_h \sum_{m \le M} a_{hm}(x_b) R_{hm\to gn}(x_b \to x) \tag{10}$$

Note that the above equation is exact if all values of m, the order of the DLP in Eq. (8), are considered. Our intention, however, is to reduce the range of m and still achieve a very good approximation of ψ.

Before proceeding, it should be noted that our response formulation is rather different than the conventional ones (*e.g.*, [1-4]), regardless of the choice of intra-nodal expansion. In the conventional methods, a node is characterized by solutions to fine mesh, fixed source problems with *no fission source*. Consequently, responses to both node-edge incident fluxes and in-volume sources are required, which leads to a greater number of response functions. On the other hand, the global eigenvalue is generally not known *a priori*, so our approach requires iterations on the eigenvalue.

3. COARSE MESH METHOD IN 1-D

The numerical coarse mesh method involves both inner (flux update) and outer (k update) iterations. These are discussed separately in the following two sub-sections.

3.1. Inner Iterations

The goal of the inner iterations is to converge an estimate of the global flux solution associated with the latest eigenvalue guess. The basic step of the flux update algorithm is the calculation of the angular fluxes exiting each side of a single coarse mesh using the latest available estimate of the incident fluxes and response functions. This process is illustrated schematically in Figure 1.

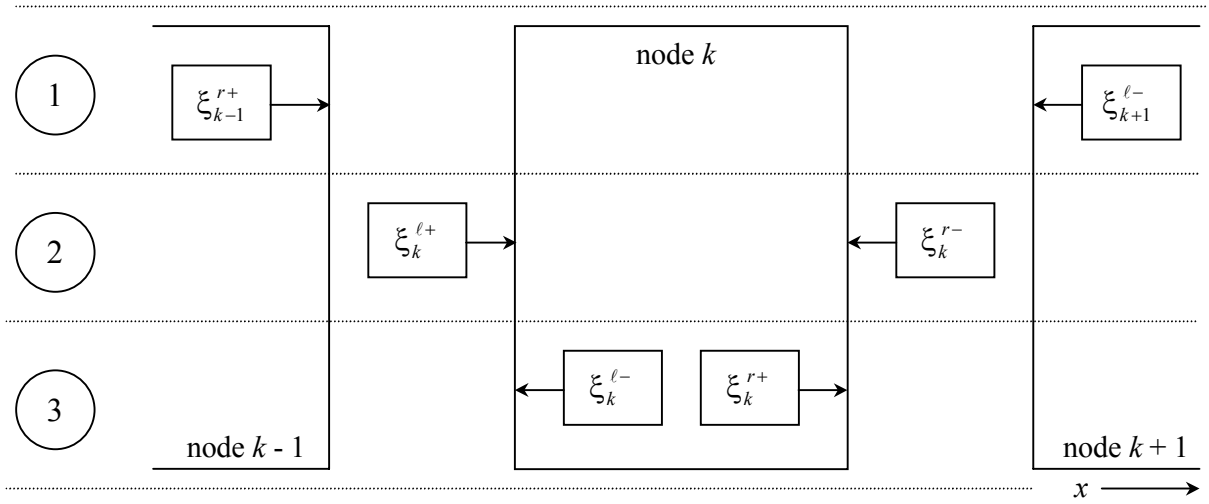

Figure 1. Basic Inner Iteration Step

The figure shows an arbitrary node, denoted k, and its neighbors to the left and right, nodes $k-1$ and $k+1$, respectively. These nodes are all adjacent, however a gap was drawn between them so that the different quantities of interest could be clearly represented. The quantity denoted $\xi_k^{\ell+}$, for example, is the angular flux entering the left edge of coarse mesh k with group and ordinate subscripts suppressed. If node k happens to lie adjacent to the left external boundary, for example, then ξ_{k-1}^{r+} denotes the return angular flux from the boundary condition.

As noted in the figure, the so-called basic step has three parts. First, two sets of expansion coefficients up to order $M_u \leq M$ (a user-defined parameter) are calculated using the most recent estimates of ξ_{k-1}^{r+} and $\xi_{k+1}^{\ell-}$ in Eq. (9). Note that this implies that initial guesses are required for the angular flux entering each coarse mesh, except where vacuum or known incident flux boundary conditions are imposed. Second, the quantities $\xi_k^{\ell+}$ and ξ_k^{r-} are calculated using a relationship which follows from Eq. (9)

$$\xi_{hn}(x_b) = \sum_{m=0}^{M_u} a_{hm}(x_b) P_m(n-t, \frac{N}{2}-1) \tag{11}$$

Note that for $M_u < M$, it will generally be the case that $\xi_k^{\ell+} \neq \xi_{k-1}^{r+}$ and $\xi_k^{r-} \neq \xi_{k+1}^{\ell-}$ because some detailed information has been lost. Integral information, specifically the partial currents associated with

ξ_{k-1}^{r+} and $\xi_{k+1}^{\ell-}$, however, can be preserved. For example, at the left edge of node k, the expansion coefficients are multiplied by the factor

$$c_k^{\ell} = \frac{\sum_n w_n \mu_n \xi_{k-1}^{r+}}{\sum_n w_n \mu_n \xi_k^{\ell+}} \tag{12}$$

where n is restricted so that $\mu_n > 0$. The expansion coefficients on the right edge are similarly adjusted, and new values of $\xi_k^{\ell+}$ and ξ_k^{r-} are computed. In the third and final part, the exiting fluxes, $\xi_k^{\ell-}$ and ξ_k^{r+}, and the intra-nodal flux are calculated according to Eq. (10).

A complete inner iteration consists of performing the basic step for each coarse mesh in the system. The inner iterations are continued until the following pointwise convergence criterion is achieved

$$\max \left| \frac{\psi_{ign}^{(j+1)} - \psi_{ign}^{(j)}}{\psi_{ign}^{(j)}} \right| < \epsilon_{inner} \tag{13}$$

where i denotes a fine mesh and the superscripts denote iteration indices.

When $M_u < M$, the converged global flux distribution depends on the order in which the coarse meshes are treated due to the approximate representation of the angular fluxes transmitted across node interfaces. For example, the converged flux in a symmetric problem will generally not be symmetric if the meshes are treated from left to right (or right to left) through the core, because information is not lost in a symmetric fashion. We have found two procedures that do not have this problem. In a seven assembly core, the two procedures progress through the nodes (numbered from left to right) according to

$$1 \rightarrow 2 \rightarrow 3 \rightarrow 7 \rightarrow 6 \rightarrow 5 \rightarrow 4 \quad (\textit{outside-in})$$

$$4 \rightarrow 3 \rightarrow 2 \rightarrow 1 \rightarrow 5 \rightarrow 6 \rightarrow 7 \quad (\textit{inside-out})$$

The most recent values of the incident fluxes are always used in the first part of the basic step. The results presented in Section 4 were generated using the outside-in procedure.

3.2. Outer Iterations

The goal of the outer iterations is to compute an estimate of k using the latest global flux estimate. The eigenvalue can be computed from a simple neutron balance (absorption and leakage divided by production), or by variational techniques. In this work, we have used a Rayleigh quotient that is derived by simply rearranging the variational principle in [6] to isolate the eigenvalue. The Rayleigh quotient leads to a more accurate final (converged) estimate of k than the neutron balance relation when an incomplete set of response functions is used. On the other hand, adjoint response functions and (at the current stage of development) a global adjoint flux estimate have to be generated. The latter is computed in a completely analogous procedure to the one previously discussed for the forward flux estimate.

As in the conventional fine mesh methods, eigenvalue iterations continue until the following convergence criterion is satisfied

$$\left| k^{(j+1)} - k^{(j)} \right| < \epsilon_{outer} \tag{14}$$

4. NUMERICAL RESULTS

In previous work, three one-dimensional core configurations were adapted from those published in [12]. The cores contain the four unique assembly designs presented in Table II. There, the regions are numbered from left to right, and each one contains a single homogeneous material characterized by the one group macroscopic cross sections presented in Table III. The core loading patterns are presented in Table IV, with assembly positions numbered from left to right. Note that the compositional heterogeneity increases from configuration 1 to 2 and from 2 to 3. To see this, compare the infinite multiplication factors, k_∞, of adjacent assemblies (see Table II). Reference solutions were computed using one spatial node per region and vacuum boundary conditions. S_{12} quadrature was chosen for no reason other than it leads to a convenient number of total response functions (six per coarse mesh, due to symmetry) for this stage of development. The reference k's are shown in Table IV.

Table II. Assembly Designs

Region	Width (cm)	Type A $k_\infty = 1.25$	Type B $k_\infty = 1.39$	Type C $k_\infty = 0.80$	Type D $k_\infty = 0.19$
1, 6	1.158	Water	Water	Water	Water
2, 5	3.321	Fuel 1	Fuel 1	Fuel 1	Fuel + Gd
3, 4	3.321	Fuel 2	Fuel 1	Fuel + Gd	Fuel + Gd

Table III. Material Cross Sections (1/cm)

	Water	Fuel 1	Fuel 2	Fuel + Gd
σ	0.1890	0.2263	0.2252	0.2173
σ_0	0.1557	0.2006	0.1994	0.1902
$\nu\sigma_f$	0	0.04285	0.0345	0.006122

Table IV. Core Configurations

Position	Conf. 1 $k_{ref} = 1.26784$	Conf. 2 $k_{ref} = 1.00729$	Conf. 3 $k_{ref} = 0.83823$
1, 3, 5, 7	Type A	Type A	Type A
2, 4, 6	Type B	Type C	Type D

For these problems, we set a target accuracy of 1% relative error in the pin power predictions

$$\max \left| \frac{P_i^{est} - P_i^{ref}}{P_i^{ref}} \right| \leq 0.01 \tag{15}$$

where i denotes a fine mesh containing fissionable material. Of particular interest is the expansion order M_u, which is the upper limit of m in Eqs. (4 and 11), required to achieve the accuracy goal with both intra-nodal flux expansion ideas. Since these problems involve one-group cross sections, S_{12} quadrature, and symmetric fuel assemblies, a complete set of response functions contains six members. In other words, a 5^{th} order expansion results in no loss of information.

For the first core configuration, the convergence of the numerical procedure using SGFs (our original expansion) is presented in Table V. Starting with the 3^{rd} order SGF expansion and a guess of $k = 1$ the process described in Section 3 was executed until the convergence criterion $\epsilon_{outer} < 1 \times 10^{-5}$ was reached after five outer iterations. The maximum pin power error at this point (6.40%) did not meet the accuracy requirement, so a 4^{th} order expansion was used with the eigenvalue from the 5th outer iteration. Convergence was again reached after three additional iterations (in outer iteration 8). Not surprisingly, a 5^{th} order expansion (*i.e.*, a complete response function set) was required to reach the accuracy target in the end. The performance of the SGF expansion is worse in the other two core configurations, and so no additional SGF results are presented.

Table V. Results for Core Configuration 1 Using Surface Green's Functions

Expansion Order	Outer Iteration	Initial k_{eff}	Maximum Pin Power % RE	Final k_{eff}	k_{eff} % RE
3	1	1.00000	52.45	1.18849	-6.26
	2	1.18849	11.85	1.27058	0.22
	3	1.27058	5.27	1.27755	0.77
	4	1.27755	6.38	1.27771	0.78
	5	1.27771	6.40	1.27772	0.78
4	6	1.27772	2.85	1.26891	0.08
	7	1.26891	1.46	1.26884	0.08
	8	1.26884	1.46	1.26884	0.08
5	9	1.26884	0.16	1.26784	0.00
	10	1.26784	0.00	1.26784	0.00

Results for the discrete Legendre polynomial RF expansion are presented in Tables VI - VIII. The maximum pin power error in the converged 0^{th} order solution increases with the heterogeneity of the system, from 1.56% to 4.67%. In every case, the addition of 1^{st} order response functions leads to errors substantially less than 1%.

Table VI. Results for Core Configuration 1 Using DLP Response Functions

Expansion Order	Outer Iteration	Initial k_{eff}	Maximum Pin Power % RE	Final k_{eff}	k_{eff} % RE
0	1	1.00000	56.62	1.19123	-6.04
	2	1.19123	12.78	1.26468	-0.25
	3	1.26468	1.85	1.26768	-0.01
	4	1.26768	1.56	1.26764	-0.02
	5	1.26764	1.56	1.26764	-0.02
1	6	1.26764	0.19	1.26783	-0.001
	7	1.26783	0.21	1.26783	-0.001

Table VII. Results for Core Configuration 2 Using DLP Response Functions

Expansion Order	Outer Iteration	Initial k_{eff}	Maximum Pin Power% RE	Final k_{eff}	k_{eff} % RE
0	1	1.00000	3.19	1.00714	-0.01
	2	1.00714	3.19	1.00714	-0.01
1	3	1.00714	0.27	1.00727	-0.002
	4	1.00727	0.28	1.00727	-0.002

Table VIII. Results for Core Configuration 3 Using DLP Response Functions

Expansion Order	Outer Iteration	Initial k_{eff}	Maximum Pin Power % RE	Final k_{eff}	k_{eff} % RE
0	1	1.00000	46.54	0.81288	-3.02
	2	0.81288	13.28	0.83681	-0.17
	3	0.83681	4.67	0.83798	-0.03
	4	0.83798	4.67	0.83798	-0.03
1	5	0.83798	0.60	0.83821	-0.003
	6	0.83821	0.54	0.83821	-0.003

5. CONCLUSIONS

A new intra-nodal angular flux expansion was developed for a heterogeneous coarse-mesh discrete ordinates method. A new inner iteration algorithm for converging the global flux estimate was also developed. The numerical method was tested using three one-speed, one-dimensional slab geometry cores with varying degrees of heterogeneity. The original expansion technique required six response functions per node (a complete set) to achieve the target pin power accuracy ($\leq$ 1% relative error). With the new technique, only two response functions per node (1^{st} order expansion) were required to achieve pin power errors of less than 0.6% and eigenvalue errors of less than 0.005%.

6. FUTURE WORK

Before extending the coarse mesh method to 2-D Cartesian geometry, a different variational approach will be investigated. Specifically, finite element equations can be derived by substituting the expansion in Eq. (10) into the variational principle from [6]. Solving these equations should lead to angular flux and eigenvalue estimates accurate to second order in the trial function error. This is an improvement over the technique described in this paper, in which only the eigenvalue has second order accuracy. If the finite element technique can reduce the number of outer iterations required to achieve a fixed degree of accuracy, then additional savings in computational time will be obtained.

ACKNOWLEDGMENTS

The authors gratefully acknowledge the support of this work by the U.S. Department of Energy's Nuclear Energy Research Initiative (NERI) under contract number DE-FG03-02SF22619, NERI Grant 2002-081.

REFERENCES

[1] E.A. Villarino and R.J.J. Stamm'ler, "The Heterogeneous Response Method in Slab Geometry," *Ann. Nucl. Energy*, **11**, pp. 429-440 (1984).

[2] J.A. Rathkopf and W.R. Martin, "The Finite Element Response Matrix Method for the Solution of the Neutron Transport Equation," *Prog. Nucl. Energy*, **18**, pp. 237-250 (1986).

[3] M.A. Smith, N. Tsoulfanidis, E.E. Lewis, G. Palmiotti, and T.A. Taiwo, "Whole-Core Neutron Transport Calculation without Fuel-Coolant Homogenization," *Proc. Int. Mtg. Advances in Reactor Physics and Mathematics and Computation into the Next Millennium*, Pittsburgh, Pennsylvania, May 7-11 (2000).

[4] M. Tsuiki and S. Hval, "A Variational Nodal Expansion Method for the Solution of Multigroup Neutron Diffusion Equations with Heterogeneous Nodes," *Nucl. Sci. Eng.*, **141**, pp. 218-235 (2002).

[5] E.M. Nichita and F. Rahnema, "A Heterogeneous Finite Element Method in Diffusion Theory," *Ann. Nucl. Energy*, **30**, pp. 317-347 (2003).

[6] D. Ilas and F. Rahnema, "A Heterogeneous Coarse Mesh Transport Method," to appear in *Transp. Theory Stat. Phys.* (2003).

[7] K.S. Smith, "Assembly Homogenization Techniques for Light Water Reactor Analysis," *Prog. Nucl. Energy*, **17**, pp. 303-335 (1986).

[8] R.D. Lawrence, "Progress in Nodal Methods for the Solution of the Neutron Diffusion and Transport Equations," *Prog. Nucl. Energy*, **17**, 271-301 (1986).

[9] E.E. Lewis and W.F. Miller, Jr., *Computational Methods of Neutron Transport*, American Nuclear Society, La Grange Park, Illinois, USA (1984).

[10] K.M. Case and P.F. Zweifel, *Linear Transport Theory*, Addison-Wesley, Reading, Massachusetts, USA (1967).

[11] C.P. Neuman and D.I. Schonbach, "Discrete (Legendre) Orthogonal Polynomials - A Survey," *Intl. J. Num. Meth. Engr.*, **8**, pp. 743-770 (1974).

[12] R.T. Chiang, "A Lattice Homogenization Theory for Coarse Mesh Diffusion Analysis," *Proc. Tpl. Mtg. Advances in Reactor Physics and Thermal Hydraulics*, Kiamesh Lake, NY, September 22-24, Vol. 1, pp. 391-405 (1982).